Graphical approach to the U(n) Racah-Wigner theory of angular momentum

R. D. Kent
School of Computer Science, University of Windsor, Windsor, Ontario, Canada N9B 3P4

M. Schlesinger
Department of Physics, University of Windsor, Windsor, Ontario, Canada N9B 3P4
(Received 1 March 1989)

We demonstrate the use of angular momentum graphs, based on those of Yutsis, Levinson, and Vanagas [*Mathematical Apparatus of the Theory of Angular Momentum* (Israel Program for Scientific Translation, Jerusalem, 1962)], adapted for the unitary group approach to the theory of many-particle systems. Using a variant of the standard Gel'fand state labels, we show that graphical representations of generator matrix elements in U(n) parallel the SU(2) vector-coupling approaches of Drake and Schlesinger [Phys. Rev. A **15**, 1990 (1977)] and Paldus and Boyle [Phys. Scr. **21**, 295 (1980)]. The graphs are constructed using the U(n) Clebsch-Gordan coefficients. Fundamental subgraphs, such as occur in the evaluation of operator matrix elements, are expressed in terms of U(n) Racah coefficients and generalized $3n$-j coefficients. The results are anticipated to be of interest to high-energy physicists and to others concerned with systems of particles involving spin higher than $\frac{1}{2}$.

I. INTRODUCTION

The purpose of this paper is to present a graphical representation of many-particle symmetry-adapted states and operator matrix elements in U(n) using the vector-coupling paradigm. In our treatment we employ extensions of the graphical techniques of Yutsis, Levinson, and Vanagas[1,2] (YLV).

Early workers[3–11] showed that one can develop a theory of tensor operators in U(n) which retains the same basic features as in the SU(2) paradigm. This leads, in turn, to the generalizations of the Wigner and Racah coupling coefficients. After Baird and Biedenharn,[4] we refer to this approach as the generalized Racah-Wigner calculus.

It does not appear that the considerable computational apparatus afforded by the unitary group calculus has been exploited in U(n) [SU(n)] as it has in the case of the $U(2n)\supset U(n)\times SU(2)$ groups. In recent years a great deal of progress[12–17] has been made in the study of the latter groups applied to electronic spin orbitals (see Ref. 16 for an extensive list of contributors prior to 1979). Of particular significance to the current work are the papers of Shavitt[14] who developed an efficient method for generating and representing the complete basis for a given U(n) irreducible representation (irrep) and Drake and Schlesinger[13] and Paldus and Boyle[15] in which the application of the YLV spin graphs provided considerable insight into the structure of the matrix elements of the generators.

In a recent sequence of papers[18,19] we have extended many of these basic improvements to general permutation symmetry adapted many-particle systems. Specifically, we presented methods for labeling and generating the N-particle basis functions of unitary permutational symmetry adapted irreducible representations [$U(n)\downarrow S_N$ irreps] and for calculating the matrix elements of the U(n) generators [$E_{\mu,\nu}$] in this many-particle basis. Further to the last point we emphasize that in addition to the factorized products, which arise in the single generator matrix elements, we derived similar expressions for multigenerator product matrix elements also.

The approach we adopt includes the following steps as they are presented in the paper. We give a review of basic theory and introduce notation in Sec. II. In Sec. III we express the generator matrix elements in terms of YLV graphs and demonstrate methods for decomposing these into fundamental subgraphs which are related to the Racah coefficients. In Sec. IV the methods are further extended to treat cases of matrix elements of generator products, utilizing graphs corresponding to the generalized $3n$-j coefficients. Section V contains remarks of a more general nature concerning the SU(2) limit and areas of potential application.

II. THEORY AND NOTATIONS

Orthonormal bases of the irreducible representations (irreps) of U(n) may be constructed[3] by adapting appropriate labels to the group chain

$$U(n)\supset U(n-1)\supset \cdots \supset U(\tau)\supset \cdots \supset U(1) . \quad (2.1)$$

The state labels are the integer partitions $m_{\rho\tau}$; $\rho=1,\ldots,\tau$; $\tau=1,\ldots,n$. States are expressed recursively[4] by the Gel'fand tableaux,

$$|(m)_n\rangle = \left| \begin{Bmatrix} [m_n] \\ (m)_{n-1} \end{Bmatrix} \right\rangle ,$$

$[m_\tau]$ denoting the vector whose elements are $m_{\rho\tau}$. These labels satisfy the so-called betweenness (lexicality) conditions $m_{\rho\tau}\geq m_{\rho\tau-1}\geq m_{\rho+1\tau}$.

In the case of N-particle systems it proves useful to adopt an alternative (equivalent) specification of Gel'fand states by adapting to the group chain[10]

$$S_N \supset S_{N_{n-1}} \supset \cdots \supset S_{N_\tau} \supset \cdots \supset S_{N_1} , \tag{2.2}$$

where N_τ is the number of single-particle (SP) states labeled $|n\tau\rangle (N \equiv N_n)$. The appropriate labels are the S_N partition labels. States of U(n) are represented using the Weyl basis.

In Refs. 18 and 19 we reported on the use of S_N labels to represent the irreps of U(n) consistent with the Weyl branching law. Additionally, we determined algebraic expressions for generator matrix elements. This scheme is referred to as the distinct row table (DRT) or graphical unitary group approach (GUGA). Chen and coworkers[20] have also reported recent progress using the symmetric group approach to obtain algebraic expressions and presented tables[21] for U(n) Clebsch-Gordan, Racah, and subduction coefficients. In the current paper we attempt to unify several aspects of these different approaches.

In general the Gel'fand labels may be positive, zero, or negative. One can construct a one-to-one mapping[10] between the Gel'fand and Weyl tableau representation by restricting attention to non-negative $m_{\rho\tau}$. Assume $m_{1n}=L$, the number of boxes in the top row of the Weyl tableau corresponding to $[m_n]$. It follows (from the betweenness conditions) that $m_{\rho\tau} \le L$. We can recast the $[m]_\tau$ in terms of a new vector p_τ whose elements $p_{\tau k}$, $k=0,\dots,L$ are the number of $m_{\rho\tau}=k$ for each τ. The vector p_τ prescribes the partition $[L^{p_{\tau L}} \cdots k^{p_{\tau k}} \cdots 0^{p_{\tau 0}}]$ of $N_\tau = \sum_{k=0}^{N} k p_{\tau k}$. The p_τ values are restricted by the betweeness conditions.

We rewrite states in the recursive form

$$|N(p)_n\rangle = \left| \begin{Bmatrix} N_n r_n p_n \\ N_{n-1}(p)_{n-1} \end{Bmatrix} \right\rangle ,$$

where $r_\tau = N_\tau - N_{\tau-1}$ are the number of SP states $|n\tau\rangle$. Note that the Weyl frame shape after the coupling of all $\rho \le \tau$ SP states is specified by $p_{\tau k}$, $1 \le k \le L$; these labels specify N_τ. In order to specify uniquely the r_τ positions of each τ labeled box in the Weyl tableau, one requires both the p_τ and $p_{\tau-1}$ vectors. Clearly, N_τ and r_τ are redundant for a given p_τ:$p_{\tau-1}$ couple. Nonetheless, we retain these labels and interpret the p_τ as representatives of the projections of N_τ. In this sense p_τ are analogous to projection labels m in the case of j (l or s) states in SU(2); usually p_τ are treated like j, however. The emphasis on the j-m analogy is intended to promote an understanding that, although the SU(2) formalism is a special case of U(n), the more general group presents no radically new concepts and, further, utilizes an algebra and other computational tools which are extensible to groups of all orders.

Consider a Weyl tableau (S_{N_τ} partition) $p_{\tau-1}$ to which are coupled r_τ boxes labeled τ. The rules for expressing this coupling may be stated as the following: add the boxes in all ways such that no two boxes are in the same column and all boxes are contiguous within rows. The maximum number of ways of adding boxes is just ${}^LC_r = L!/r!(L-r)!$ (realized when $p_{\tau-1k} \neq 0\ \forall k$). For $r_\tau = 0,1,\dots,L$ this gives $\sum_{r=0}^{L} {}^LC_r = 2^L$ different possible arrangements. For each of the resulting tableaux $p_\tau^{(t)}$, $t=0,\dots,2^L-1$, we define difference vectors

$$d_\tau^{(t)} = p_\tau^{(t)} - p_{\tau-1}, \quad \sum_{k=0}^{L} d_{\tau k}^{(t)} = 1, \quad 0 \le t \le 2^L - 1 . \tag{2.3}$$

We note that the definition of $d_\tau^{(t)}$ does not depend on the labels τ and $\tau-1$, rather, only on the difference between frame shapes. We shall specify the index t only when ambiguities may arise.

We separately couple the r_τ SP states $|n\tau_i\rangle, i=1,\dots,r_\tau$ into a (one-dimensional) symmetric state of U(1) and S_{r_τ}, abbreviated to $|[r_\tau]\rangle \equiv |[r_\tau^1]\rangle$. The difference vectors specify unique projections $|r_\tau d_\tau\rangle$ of $|[r_\tau]\rangle$ in a nonstandard basis[22] in which the particle position indices i map (one-to-one) into $c_i \le L$ $(\tau_i \rightarrow \tau_{c_i})$. By imposing the restriction $\langle n\tau_{c_i} | n\tau_{c_j}\rangle = \delta_{i,j}$, the $|r_\tau d_\tau\rangle$ can be made orthonormal.

This notation also suggests a method of enumerating states (boxes) in a Weyl tableau. We construct a tableau by first adding all 1 boxes ($|n1\rangle$), then 2's and so on, up to boxes labeled n. We further adopt the convention that all boxes labeled τ are counted from left to right. By adopting this construction convention it follows that the Weyl basis is orthonormal and that each fully labeled Weyl tableau corresponds uniquely to a Gel'fand tableau. Each state can also be ordered lexically relative to other states using the Yamanouchi[20] convention.

Next, we define the components of the vector ∂_λ

$$\begin{aligned} &\partial_\lambda^i = (-1)^{i-1}\partial_\lambda , \\ &\partial_{\lambda k}(\lambda) = \delta_{k,\lambda} - \delta_{k,\lambda-1} , \\ &i=1,2, \quad 1 \le \lambda \le L \end{aligned} \tag{2.4}$$

where λ is referred to as the pivot index. We refer to a vector sum by ∂_τ^i as a creation ($i=1$) or annihilation ($i=2$) shift. The sense of this terminology is seen by noting first that

$$\begin{aligned} &\sum_{k=1}^{L} k d_{\tau k} = r_\tau , \\ &\sum_{k=1}^{L} k \partial_{\tau k}^i = \begin{cases} 1, & i=1 \\ -1, & i=2 \end{cases} \end{aligned} \tag{2.5}$$

whereupon it follows that in the transformation $d_\tau \rightarrow d'_\tau = d_\tau \pm \partial_\tau$, one increments (+) [decrements (−)] the number of τ labeled SP states by 1. The pivot index specifies the column of a Weyl tableau in which a box labeled τ is changed to $\tau \pm 1$ (by the action of a generator). We shall suppress the pivot index unless required to avoid ambiguity. We also note that application of ∂ ($-\partial$) is equivalent to a left (right) coset decomposition of the Yamanouchi-Kotani basis as described by Sarma and Sahasrabudhe[22] and by Chen *et al.*[20] We shall now define a pseudo-vector-coupling scheme using N, r, p, d and ∂.

The coupling of a symmetric state $|[r_\tau]\rangle$ to the state

$|N_{\tau-1}(p_{\tau-1})\rangle$ to form a resultant state $|N_\tau(p_\tau)\rangle \equiv |N_\tau r_\tau(p_\tau)\rangle$ will be expressed as

$$|N_{\tau-1}(p_{\tau-1})\rangle \otimes |[r_\tau]\rangle = \sum_{d_\tau} |N_\tau r_\tau(p_\tau)\rangle \times \langle N_\tau p_\tau | N_{\tau-1} r_\tau p_{\tau-1} d_\tau \rangle \ , \tag{2.6}$$

$$|N_\tau r_\tau(p_\tau)\rangle = \sum_{d_\tau} |N_{\tau-1}(p_{\tau-1})\rangle \otimes |[r_\tau]\rangle \times \langle N_\tau p_\tau | N_{\tau-1} r_\tau p_{\tau-1} d_\tau \rangle \ , \tag{2.7}$$

where $\langle N_\tau p_\tau | N_{\tau-1} r_\tau p_{\tau-1} d_\tau \rangle$ in (2.6) is viewed either as the $U(\tau)\downarrow U(1)\otimes U(\tau-1)$ Clebsch-Gordan coefficient (CGC) or the $S_{N_\tau}\downarrow S_{r_\tau}\otimes S_{N_{\tau-1}}$ subduction coefficients. The equivalent interpretations result from the multiplicity free[20] nature of the coupling. Further, it follows that the CGC's are zero unless the selection conditions $N_\tau = N_{\tau-1} + r_\tau$ and $p_\tau = p_{\tau-1} + d_\tau$ are satisfied. Relation (2.7) introduces the CGC of the induced representations $S_{r_\tau}\otimes S_{N_{\tau-1}}\uparrow S_{N_\tau}$ which are equal to the subduction CGC (from the Frobenius reciprocity theorem).

The labels p_τ serve a dual role in the remainder of the paper. In the case of the CGC they are viewed as projection (m) labels; however, with respect to Racah coefficients, as will be shown, they are used to represent irrep labels (j). To each of the CGC's we assign graphs in the manner of Yutsis, Levinson, and Vanagas.[1,2]

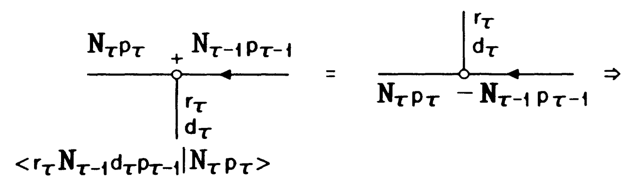

FIG. 1. YLV graphs corresponding to the CGC.

As shown in Fig. 1 the YLV graph denoting the CGC $\langle r_\tau N_{\tau-1} d_\tau p_{\tau-1} | N_\tau p_\mu \rangle$ is specified by three lines joined at a single node. We adopt the convention, in conformity with the induction $S_{N_{\tau-1}}\otimes S_{r_\tau}\uparrow S_{N_\tau}$, that the line labeled $p_{\tau-1}$ carries an arrow directed toward the node. The lines labeled r_τ and p_τ carry no arrow, but the node has a plus sign attached to it and the lines $p_{\tau-1}$, r_τ, and p_τ are oriented clockwise relative to each other. A change in orientation of the lines, corresponding to the adjoint CGC, results in the same CGC provided the node sign changes to minus; otherwise, the appropriate phase choice regarding juxtaposition of CGC labels must be incorporated.

From the orthonormality of the states it follows that the CGC's satisfy unitarity conditions

$$\sum_{p_\tau} \langle N_\tau r_\tau p_\tau | N_{\tau-1} r_\tau p_{\tau-1} d_\tau \rangle \langle N_\tau r_\tau p_\tau | N_{\tau-1} r_\tau p'_{\tau-1} d'_\tau \rangle = \delta_{p_{\tau-1}, p'_{\tau-1}} \delta_{d_\tau, d'_\tau} \ , \tag{2.8}$$

$$\sum_{p_{\tau-1}} \sum_{d_\tau} \langle N_\tau r_\tau p_\tau | N_{\tau-1} r_\tau p_{\tau-1} d_\tau \rangle \langle N_\tau r_\tau p'_\tau | N_{\tau-1} r_\tau p_{\tau-1} d_\tau \rangle = \delta_{p_\tau, p'_\tau} \ . \tag{2.9}$$

We shall ignore for the present the overall phase conventions. Relative phases, which are important, will be discussed, however.

Each fully coupled basis vector $|N(p_n)\rangle$ is represented graphically as shown in Fig. 2. The coupling results from joining lines p_μ $(\mu = 1, \ldots, n-1)$ at each level μ. The adjoint vectors $\langle N(p)_n|$ are represented by graphs conjugate to those above; lines labeled r_τ branching upward from the p-labeled spine and the sign on each node changes to minus.

Finally, when all SP states have been coupled according to the scheme described above, the permutation symmetry corresponding to each irrep chain (p_n) is achieved by the application of the appropriate Young operator. Thus,

$$|N(p)_n\rangle = \prod_{\tau=1}^{n} \langle r_\tau N_{\tau-1} d_\tau p_{\tau-1} | N_\tau p_\tau \rangle (N!)^{-1} \sum_{\pi\in p_n} (-1)^\pi \prod_{\lambda=1}^{n} |[r_\lambda]\rangle \ , \tag{2.10}$$

where the sum over π denotes the $N!$ permutations and $(-1)^\pi$ accounts for even $[\mathrm{mod}_2(\pi)=0]$ and odd $[\mathrm{mod}_2(\pi)=1]$ permutations.

Consider two different inductions $S_{r_\tau}\otimes S_{N_{\tau-1}}\uparrow S_{N_\tau}$ and $S_{r'_\tau}\otimes S_{N'_{\tau-1}}\uparrow S_{N_\tau}$ each coupled to the same irrep p_τ. The coupling orders can be related through the $U(n)$ Racah coefficients. For instance, we employ the Racah coefficient

$$R(p_{\tau-1} r_\tau p'_{\tau-1} r'_\tau ; p_\tau 1) = \sum_{d_\tau d'_\tau \partial_\tau} \langle r_\tau N_{\tau-1} d_\tau p_{\tau-1} | N_\tau p_\tau \rangle \langle r'_\tau N_\tau d'_\tau - p_\tau | N'_{\tau-1} - p'_{\tau-1} \rangle \times \langle 1 r_\tau - \partial_\tau d_\tau | r'_\tau d'_\tau \rangle \langle 1 N'_{\tau-1} - \partial_\tau p'_{\tau-1} | N_{\tau-1} p_{\tau-1} \rangle \ . \tag{2.11}$$

The Racah coefficient in (2.11) is equal to $U(r'_\tau 1 p_\tau p_{\tau-1}; r_\tau p'_{\tau-1})$ as defined by Chen *et al.*[21] The YLV graph for $R(p_{\tau-1} r_\tau p'_{\tau-1} r'_\tau ; p_\tau 1)$ is given in Fig. 3.

Before completing this section we relate the current approach to that of Sarma and Sahasrabudhe[22] and Chen *et al.*[20,21] In their extended Yamanouchi-Kotani scheme the number of SP states $|n\tau\rangle$ is f_τ; the number of τ states in row ρ of a Weyl tableau is $f_{\rho\tau} = m_{\rho\tau} - m_{\rho\tau-1}$ ($m_{\rho\tau}$ are

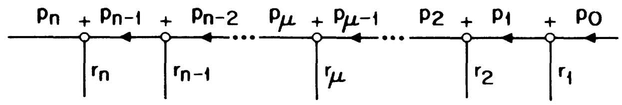

FIG. 2. Complete YLV graph corresponding to the state $|N(p_n)\rangle$.

Gel'fand labels) and $f_\tau=\sum_{\rho=1}^{R} f_{\rho\tau}$ (R is the maximum row number). Recalling that $p_{\tau k}$ represents the number of rows in column k of a Weyl tableau, it follows that $R=\sum_{k=1}^{L} p_{nk}$. Assuming that for columns j and k, $j<k$ and $p_{\tau j}\neq 0$, $p_{\tau k}\neq 0$ and $p_{\tau i}=0 \forall j<i<k$, then for $\rho=\sum_{g=k}^{L} p_{\tau g}$ we have that $f_{\rho\tau}=k-j$. We referred to $f_{\rho\tau}$ as $\nu_\tau(\lambda,k)$ in Ref. 19 (λ is the pivot index). The difference vector d_τ is therefore a signature of $\{f_{\rho\tau}\}\in f_\tau$.

III. GRAPHICAL DECOMPOSITION TECHNIQUES

The U(n) generators $E_{\mu,\nu}$ are matrices satisfying the Lie algebra commutator relations. Matrix elements of the elementary one-step raising generators $E_{\mu-1,\mu}$ are expressed as[4,19]

$$\langle (p')_n|E_{\mu-1,\mu}|(p)_n\rangle=\Delta_0^{\mu-2}\Delta_\mu^n B_\mu(p_\mu p_{\mu-1}p'_{\mu-1}) \times A_{\mu-1}(p_{\mu-1}p'_{\mu-1}p_{\mu-2}) =(r_\mu r'_{\mu-1})^{1/2}G_\mu^1((p),(p')) , \quad (3.1)$$

where the factors Δ, A, and B were defined in Ref. 19; for ease of reference we repeat these definitions below:

$$\Delta_\alpha^\beta=\prod_{\tau=\alpha}^{\beta}\prod_{k=0}^{L}\delta(p_{\tau k},p'_{\tau k}) , \quad (3.2)$$

$$B_\tau(p_\tau p_{\tau-1}p'_{\tau-1}) =\prod_{k=0}^{L}\left[\delta_{0,p_{\tau k}}+(1-\delta_{0,p_{\tau k}})\left[\frac{h_\tau(\lambda,k)}{\hat{h}_\tau(\lambda,k)}\right]^{1/2}\right] , \quad (3.3)$$

$$A_\tau(p_\tau p'_\tau p_{\tau-1}) =\prod_{k=0}^{L}\left[\delta_{0,p_{\tau k}}+(1-\delta_{0,p_{\tau k}})\left[\frac{\hat{h}_\tau(\lambda,k)}{h_\tau(\lambda,k)}\right]^{1/2}\right] . \quad (3.4)$$

In (3.3) and (3.4), we state the definition of B when it is nonzero, that is, when the triple $p_\tau p_{\tau-1}p'_{\tau-1}$ satisfies the relations $p'_{\tau-1}=p_{\tau-1}+\partial_{\lambda_{\tau-1}}$ and both $p_{\tau-1}$ and $p'_{\tau-1}$ are valid subduced irreps of p_τ. The coefficient is zero otherwise. Similar triangle conditions hold for the triple $p_\tau p'_\tau p_{\tau-1}$ in the definition of A in (3.4).

The hooklengths $h_\tau(\lambda,k)$ and $\hat{h}_\tau(\lambda,k)=h_\tau(\lambda,k)+\epsilon_{\lambda k}\nu_\tau(\lambda,k)$ ($\epsilon_{\lambda k}=1$ if $\lambda\geq k$; -1 otherwise) are defined by the expressions

$$h_\tau(\lambda,k)=|k+1-\lambda|+\sum_{j=\min(\lambda,k)}^{\max(\lambda,k)-1} P_{\tau j} \quad (3.5)$$

$$\nu_\tau(\lambda,k)=\left[1-\delta\left[0,\sum_{j=k}^{L}(p_{\tau j}-p_{\tau-1 j})\right]\right] \times[(k-k_{\max})(1-\delta_{0,k_{\max}})] , \quad (3.6)$$

where it is assumed that $k>0$.

In (3.1) the factor $(r_\mu r'_{\mu-1})^{1/2}$ arises due to the number of ways one can decouple (annihilate) or couple (create) states μ or $(\mu-1)$.[20] The graph G_μ^1 is expressed as shown in Fig. 4. The line labeled 1 between levels $\mu-1$ and μ designates the decoupling and recoupling being performed; thus, $r'_\mu=r_\mu-1$ and $r'_{\mu-1}=r_{\mu-1}+1$. Obvious factors of 1 resulting from identities $p'_\tau=p_\tau$ for $\tau=1,\ldots,\mu-2,\mu,\ldots,$ are omitted.

The following results can be derived from the definitions of A_τ and B_τ:

$$\sum_{\lambda=1}^{L} B_\tau^2(p_\tau p_{\tau-1}p_{\tau-1}+\partial_\lambda^i)=r_\tau; \quad i=1,2 . \quad (3.7)$$

$$\sum_{\lambda=1}^{L} A_\tau^2(p_\tau p_\tau+\partial_\lambda^i p_{\tau-1})=r_\tau+1; \quad i=1,2 . \quad (3.8)$$

Relations (3.7) and (3.8) can be proven inductively. We emphasize that each of the above two relations is satisfied for both creation and annihilation shifts.

We identify the A and B terms with the following Racah coefficients:

$$B_\tau(\lambda;p_\tau p_{\tau-1}p'_{\tau-1})=r_\tau R(p_{\tau-1}r_\tau p'_{\tau-1}r'_\tau;p_\tau 1) , \quad (3.9)$$

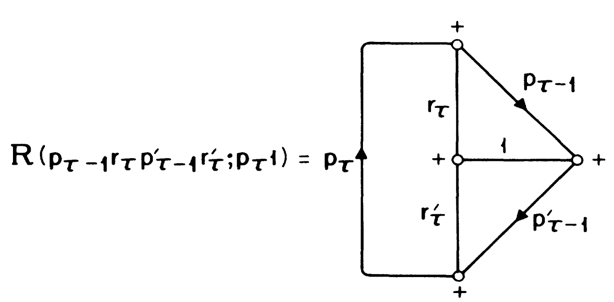

FIG. 3. YLV graph corresponding to the Racah coefficient for two different induction chains leading to the same irrep p_τ.

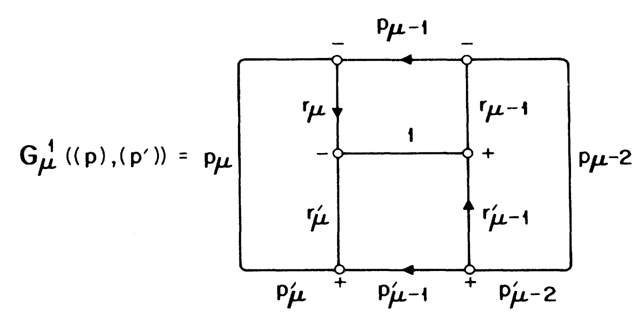

FIG. 4. Graph corresponding to a matrix element of $E_{\mu,\mu\pm 1}$.

$$A_{\tau-1}(\lambda;p_{\tau-1}p'_{\tau-1}p_{\tau-2})$$
$$=(r'_{\tau-1})^{1/2}R(p_{\tau-1}r_{\tau-1}p'_{\tau-1}r'_{\tau-1};p_{\tau-2}1) . \quad (3.10)$$

The A and B are very similar; the difference between (3.9) and (3.10) is that B (A) derives from different induction (subduction) chains leading to the same irrep p_μ ($p_{\mu-2}$). We impose the absolute phase convention that A and B, hence their corresponding R coefficients, are positive.

From the definitions (3.9) and (3.10) we determine the decomposition rule shown in Fig. 5. Cutting across the three lines at level $\mu-1$ is accomplished by inserting the identity relation

$$\sum_{i,\lambda}\langle 1N_{\mu-1}\partial^i_\lambda p_{\mu-1}|N'_{\mu-1}p'_{\mu-1}\rangle^2=1$$

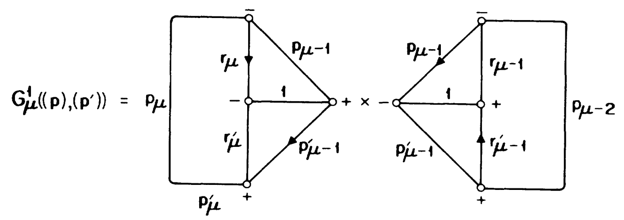

FIG. 5. Decomposition of one-step generator matrix element graph.

from (2.9) (note the sum over i and λ to account for all possible couplings) and recombining appropriate terms to form the Racah coefficients.

Next, we consider the multistep generator matrix elements which are expressed, alternatively, in algebraic [see Eq. (2.23) of Ref. 19] and graphical forms as

$$\langle(p')|E_{\mu,\nu}|(p)\rangle=B_\mu(\lambda_{\nu-1};p_\nu p_{\nu-1}p'_{\nu-1})A_\mu(\lambda_\mu;p_\mu p'_\mu p_{\mu-1})\prod_{\tau=\mu+1}^{\nu-1}T_\tau(\lambda_\tau,\lambda_{\tau-1};p_\tau p'_\tau p_{\tau-1}p'_{\tau-1})$$
$$=(r_\nu r'_\mu)^{1/2}G^1_{\mu,\nu}((p),(p')) , \quad (3.11)$$

where the graph $G^1_{\mu,\nu}$ is shown in Fig. 6. From (3.11) and the graphical decomposition in Fig. 4 we associate the central graphs with the factors T_τ which, in turn, are expressed as Racah coefficients $R(p_{\tau-1}p_\tau p'_{\tau-1}p'_\tau;r_\tau 1)$. The corresponding graph is shown in Fig. 7.

In order to determine the T_τ expressions we used previously (see Refs. 19) the Lie bracket relations $E_{\mu,\nu}=E_{\mu,\nu-1}E_{\nu-1,\nu}-E_{\nu-1,\nu}E_{\mu,\nu-1}$. We obtained the following expression:

$$T_\tau(\lambda_\tau,\lambda_{\tau-1};p_\tau p'_\tau p_{\tau-1}p'_{\tau-1})=A_\tau(\lambda_\tau;p_\tau p'_\tau p_{\tau-1})B_\tau(\lambda_{\tau-1};p'_\tau p_{\tau-1}p'_{\tau-1})-A_\tau(\lambda_\tau;p_\tau p'_\tau p'_{\tau-1})B_\tau(\lambda_{\tau-1};p_\tau p_{\tau-1}p'_{\tau-1}) . \quad (3.12)$$

Also, one can decompose the graph by inserting the CGC identity relations coupling the r_τ and 1 lines and then cutting the resulting graph across three lines taking care to ensure that all possible couplings are accounted for (both i and λ for ∂^1_λ). Equating $T_\tau(\lambda_\tau,\lambda_{\tau-1};p_\tau p'_\tau p_{\tau-1}p'_{\tau-1})=R(p_{\tau-1}p_\tau p'_{\tau-1}p'_\tau;r_\tau 1)$ we can express (3.12) in the equivalent form

$$R(p_{\tau-1}p_\tau p'_{\tau-1}p'_\tau;r_\tau 1)=\sqrt{r_\tau+1}R(p_{\tau-1}r_\tau+1p'_{\tau-1}r_\tau;p'_\tau 1)R(p_\tau r_\tau p'_\tau r_\tau+1;p_{\tau-1}1)$$
$$-\sqrt{r_\tau}R(p_{\tau-1}r_\tau p'_{\tau-1}r_\tau-1;p_\tau 1)R(p_\tau r_\tau-1p'_\tau r_\tau;p'_{\tau-1}1) . \quad (3.12')$$

This is shown in Fig. 8. The relative phase difference between the two terms in (3.12′) arises due to the fact that the number of s.p. states $|n\tau\rangle$ differs by one.

IV. TWO-BODY OPERATOR GRAPHS

In Refs. 18 and 19 we derived factorized expressions for the matrix elements of one- and two-body generators. Each factor can be decomposed into products of elementary subgraphs multiplying either a scalar or matrix term. The DRT approach suffers from a lack of elegance and efficiency in the expression of factors which are overcome using the YLV graphs. As an example, we shall rederive the matrix element expression for the two-generator product $E_{\mu\nu}E_{\mu\nu}$.

The raising-raising operator matrix element $\langle(p')|E_{\mu,\nu}E_{\mu,\nu}|(p)\rangle$ ($\mu<\nu$) is expressed as

$$\langle(p')|E_{\mu,\nu}E_{\mu,\nu}|(p)\rangle=\Delta^n_\nu\tilde{B}_\nu(\lambda^1_{\nu-1},\lambda^2_{\nu-1})\prod_{\kappa=\mu+1}^{\nu-1}\tilde{T}_\kappa(\lambda^1_\kappa,\lambda^2_\kappa,\lambda^1_{\kappa-1},\lambda^2_{\kappa-1})\tilde{A}_\mu(\lambda^1_\mu,\lambda^2_\mu)\Delta^{\mu-1}_0$$
$$=[r_\nu(r_\nu-1)r'_\mu(r'_\mu+1)]^{1/2}G^2_{\mu\nu\mu\nu}((p'),(p)) , \quad (4.1)$$

where λ^i_τ denotes the distinct pivot indices $\lambda^1_\tau<\lambda^2_\tau$ for the two shift vectors $\partial_{\lambda^i_\tau}$ operative at each level $\tau=\mu,\ldots,\nu-1$. The quantities $\tilde{B}_\nu$, $\tilde{T}_\kappa$ and $\tilde{A}_\mu$ were defined in Ref. 19 and represent 1×2, 2×2, and 2×1 matrices, respectively [the row and column are indicated by the various orders of applying the ∂ shifts, thus index 1 (2) refers to the case where ∂_{λ^1} (∂_{λ^2}) is followed by ∂_{λ^2} (∂_{λ^1}) in arriving at intermediate states].

The elements of these matrix factors are determined by combinations of B- or A-type Racah coefficients defined in (3.9) and (3.10). For instance, the elements of $\tilde{B}_\nu$ are defined as

$$\tilde{B}^{\,i}_{\nu}(\lambda^1_{\nu-1},\lambda^2_{\nu-1};p_\nu p_{\nu-1}p'_{\nu-1})=B_\nu(\lambda^i_{\nu-1};p_\nu p_{\nu-1}p_{\nu-1}+\partial_{\lambda^i_{\nu-1}})B_\nu(\lambda^{i+1}_{\nu-1};p_\nu p_{\nu-1}+\partial_{\lambda^i_{\nu-1}}p'_{\nu-1}) \tag{4.2}$$

for $i=1,2$ and the value $i+1$ in the second B factor has values of 2,1 for $i=1,2$. For the sake of brevity we shall not repeat the remaining definitions here, rather, we refer the reader to Ref. 19.

In Fig. 9 we show the reduced graph $G^2_{\mu-1\mu\mu-1\mu}$ (identities removed) for the matrix elements of $E_{\mu-1,\mu}E_{\mu-1,\mu}$. The first of the two decompositions conforms to that used to derive expressions for the factors $\tilde{B}_\mu$ and $\tilde{A}_{\mu-1}$ [see Eqs. (3.11) and (3.16) of Ref. 19]. We recall that these are row and column vector expressions, respectively. Only two terms participate in the sum indicated due to the selection rules. By utilizing matrices to account for the summations one arrives at our previous result.

In the second decomposition in Fig. 9 we adopt a different approach, first coupling the two single-particle lines (labeled 1) to all resultant irreps of S_2, namely, [2] or [1^2], and then summing over both. Figure 10 demonstrates how the graph at level μ may be decomposed into more fundamental graphs. This latter decomposition technique proves most effective in evaluating (4.1).

To see how this works we refer to the graph on the left-hand side in Fig. 10 as $\tilde{B}^{\,\prime}_\mu$ (omitting multiplicative factors of $r_\mu, r_{\mu-1}$). Although the right-hand side summation is from 1 to L, the selection rules select only two terms corresponding to the shift operators ∂_{λ^i}, $i=1,2$.

For $\xi=\lambda^i$ the product of the first and third right-hand side graphs represent $\tilde{B}^{\,i}_\mu$ in (4.2). Thus, we can define the transformation

$$\tilde{B}^{\,\prime}_\mu=\tilde{B}_\mu\mathcal{U}^{-1}(\lambda^1_{\mu-1},\lambda^2_{\mu-1}),\quad \tilde{A}^{\,\prime}_\mu=\mathcal{U}(\lambda^1_\mu,\lambda^2_\mu)\tilde{A}_\mu\ , \tag{4.3}$$

where $\mathcal{U}(\lambda^1,\lambda^2)$ is the unitary transformation matrix

$$\mathcal{U}(\lambda^1,\lambda^2)=\begin{bmatrix} \left[\dfrac{d-1}{2d}\right]^{1/2} & -\left[\dfrac{d+1}{2d}\right]^{1/2} \\ \left[\dfrac{d+1}{2d}\right]^{1/2} & \left[\dfrac{d-1}{2d}\right]^{1/2} \end{bmatrix} \tag{4.4}$$

and where $d=h_\mu(\lambda^1,\lambda^2)$ refers to the hooklength between the two boxes undergoing change of label, $\mu\rightarrow\mu-1$, in the corresponding Weyl-Young tableaux for this case.

The matrix elements $[\mathcal{U}(\lambda^1,\lambda^2)]_{ij}$, $i,j=1,2$, are the middle right-hand side graphs in Fig. 10 which can be written as the Racah coefficients $R(p_{\mu-1}1p'_{\mu-1}1;p_{\mu-1}+\partial_{\lambda^i}\alpha)$. The first and second rows of $\mathcal{U}$, considered as vectors, refer to the antisymmetric $\alpha=[1^2]$ and symmetric $\alpha=[2]$ couplings of the tableaux $|\{p\}+\partial_{\lambda^i_{\mu-1}}\rangle$, $i=1,2$, respectively (it is understood that $\partial_{\lambda^i_{\mu-1}}$ changes only the labels $p_{\mu-1}$). These hooklength expressions are precisely the expressions required to (anti-) symmetrize the state $|\{p\}\rangle$ in the labels $\mu,\mu-1$ in columns λ^1 and λ^2 of the Weyl-Young tableau. This transformation was first noted by Jahn[21] and arises in the graphical decomposition in a fundamental way through the Racah coefficients. We note that our [1^2] coupling differs from that of Chen *et al.*[21] by a minus sign; this is due to the requirement that $\mathcal{U}$ be unitary.

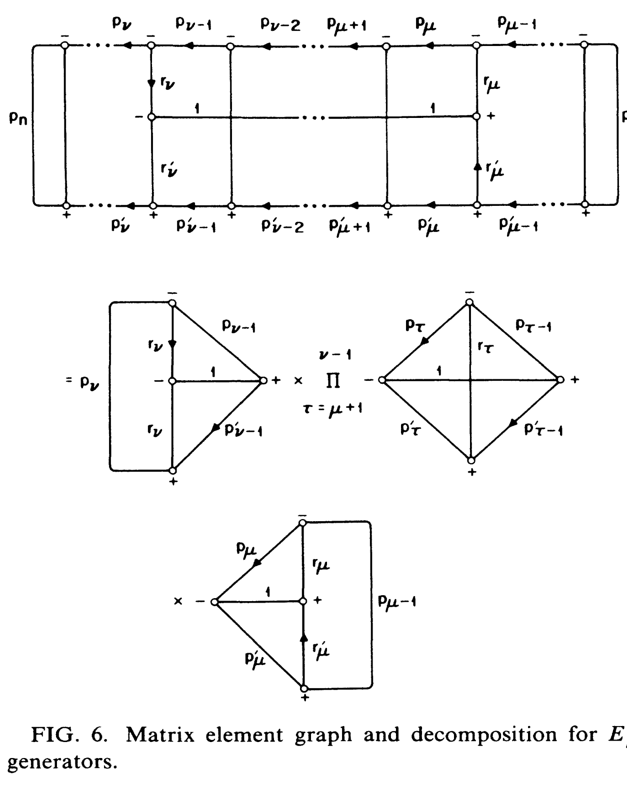

FIG. 6. Matrix element graph and decomposition for $E_{\mu,\nu}$ generators.

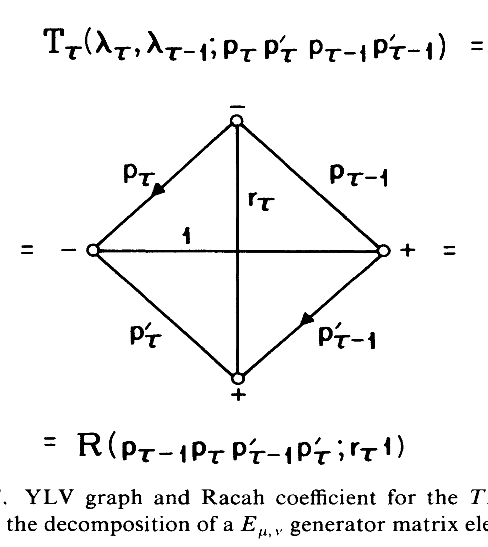

FIG. 7. YLV graph and Racah coefficient for the T_τ term arising in the decomposition of a $E_{\mu,\nu}$ generator matrix element.

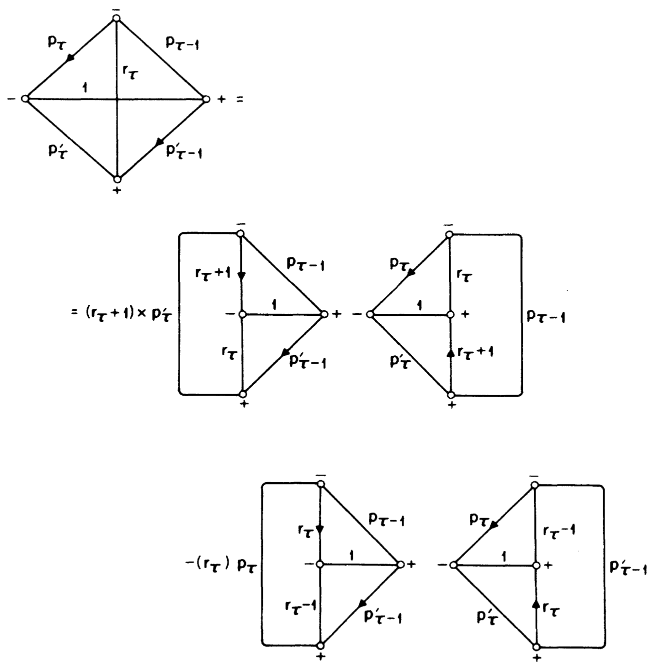

FIG. 8. Decomposition of T_τ types of graphs in terms of fundamental Racah coefficients.

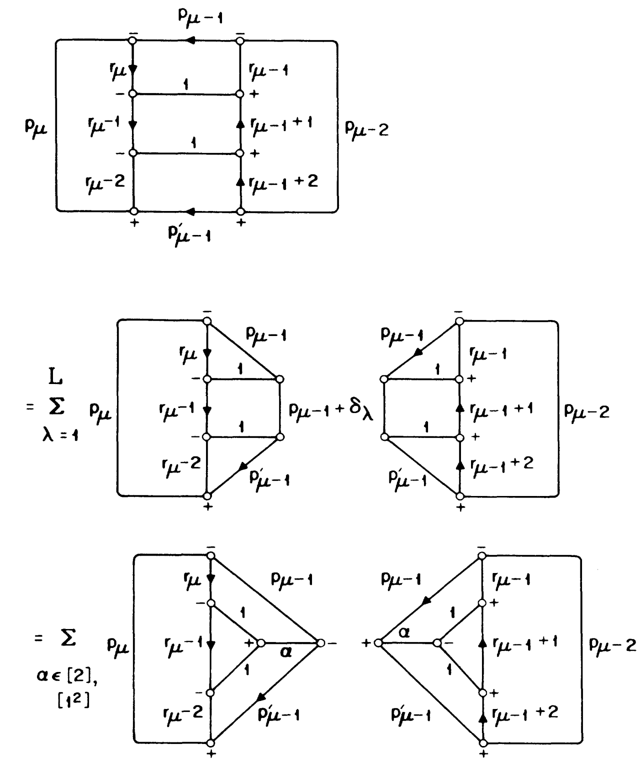

FIG. 9. Two different decompositions of $E_{\mu-1,\mu}E_{\mu-1,\mu}$ matrix element graphs.

Before proceeding we note the important result that for all off-diagonal matrix elements of two-body operators only the term arising from the symmetric coupling [2] in the overlap region contributes. It can be shown that only the [2] element of $\tilde{B}'$ ($\tilde{A}'$) is nonzero as a result of the transformation $\mathcal{U}$. The $[1^2]$ coupling contributes only for raising-lowering generator matrix elements when the bra and ket labels agree in the overlap range; in general, the $[1^2]$ coupling can be treated as a zero-angular momentum line. These properties are precisely as occurs in the SU(2) case (see Ref. 13).

The general graph $G^2_{\mu\nu\mu\nu}$ has the form shown in Fig. 11. Decomposing it by the first technique in Fig. 9 we recover all the factors displayed in (4.1) when the summation is accounted for by our matrix construction. We note, however, that this technique results in the $\tilde{T}_\tau$ matrices containing off-diagonal terms. In contrast to this the alternative decomposition, coupling the [1] irreps, results in diagonal 2×2 matrices and, thus, a more efficient approach to the matrix element computation.

One can obtain similar graphs for the various other general and special cases of raising-raising and raising-lowering generator products presented in Refs. 19.

Before continuing we note the following point concerning the $[1]\times[1]\uparrow[\alpha]$ coupling approach to graph decomposition in Fig. 12. Drake and Schlesinger[13] showed that raising-raising and raising-lowering spin graphs could be easily decomposed by first coupling the internal graph lines corresponding to the generator lines, in our case the [1] lines denoting the application of the ∂ shifts. In the SU(2) case the couplings are for two spin-$\frac{1}{2}$ particles, hence $\frac{1}{2}\times\frac{1}{2}\uparrow(0\oplus1)$ which denote singlet $S=0$ and triplet $S=1$ spin states. For U(n) there is striking similarity in that the S_2 irrep [2] ($[1^2]$) is (anti-) symmetric of dimension 1 (3) and, for the sake of analogy, can also be referred to as singlet (triplet) coupling.

V. SUPPLEMENTARY REMARKS

In this work we have deliberately attempted to maintain as much of the visual appearance of the various CGC's and Racah coefficients as developed in SU(2) in our U(n) extension. Although we have neglected the

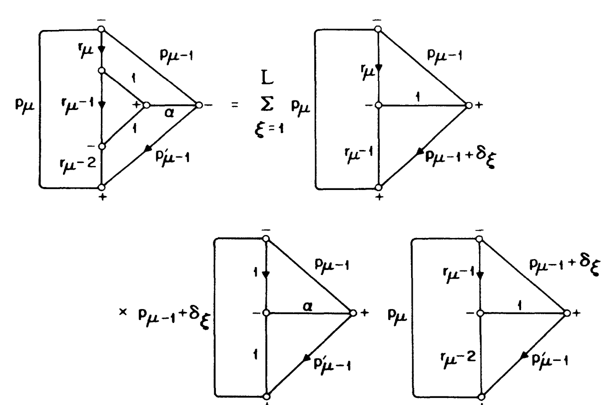

FIG. 10. Decomposition of two-body operator end graph. The irrep denoted α results from the possible couplings of $[1]\times[1]$.

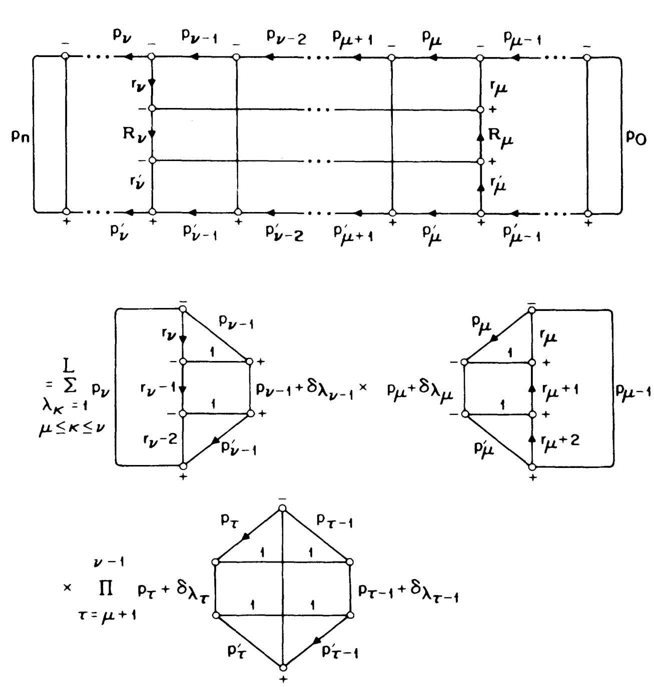

FIG. 11. Graph and one possible decomposition rule for $E_{\mu,\nu}E_{\mu,\nu}$ matrix elements.

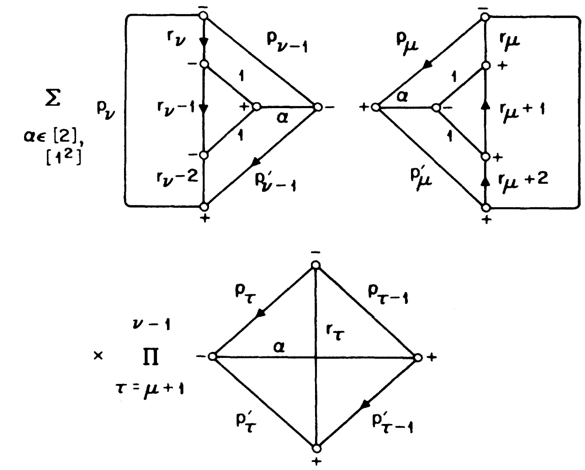

FIG. 12. A second possible decomposition rule for $E_{\mu,\nu}E_{\mu,\nu}$ matrix elements utilizing $[1]\times[1]\uparrow[\alpha]$ intermediate coupling.

matter of phases (except for relative phases where important) these can also be incorporated into the scheme following the example of SU(2) (see also Refs. 4 and 20).

Due to our state construction method it is necessary that all $U(n)$ graphs simplify to the SU(2) spin graphs obtained by either Drake and Schlesinger[13] (who neglect all trivial couplings where $r_\tau=0$) or Paldus and Boyle[15] (who constructed hole-particle states). Those graphs were intended for use in atomic and molecular modeling and configuration-interaction applications. We expect that most of the powerful techniques developed for SU(2) can be extended to $U(n)$.

In Ref. 19 we developed expressions for single-generator and two-generator product matrix elements based on the DRT and GUGA approaches. We have found that these techniques are ill suited for extension to many-generator product matrix elements. Such cases do arise and are of importance. We mention the Gel'fand invariant operators[7] and symmetry projection operators[5,23] as examples. Typical graphs which arise will include the $U(n)$ generalizations of $3n$-j coefficients. Using the decomposition rules these can be expressed in terms of simpler Racah coefficients and, thereby, explicit closed-form expressions can be derived.

Previously we reported[24] on the use of the DRT formalism to classify multiconfiguration states and calculate matrix elements for nuclear magnetic resonance (NMR). Early workers (see Louck[7] and references therein) achieved considerable success using the Gel'fand scheme in the nuclear regime. Recently Chen *et al.*[21] published tables of $SU(m+n)$ CGC's, Racah, and subduction coefficients. We applied spin graphs to mixed-configuration states[25] in order to compute the $U(2m+2n)\downarrow U(m)\otimes U(n)\otimes SU(2)$ subduction coefficients. The YLV graphical techniques can be adapted to these cases and others as well.

VI. CONCLUSIONS

In this paper we have demonstrated the extension of the SU(2) versions of the YLV spin graphs to $U(n)$. This approach provides an alternative description of the relationship between Gel'fand states and the Racah-Wigner vector-coupling approach. By viewing the N_τ partition indices p_τ as generalized vectors and defining their couping in terms of Clebsch-Gordan and Racah coefficients, one may construct a graphical realization of Gel'fand states. The extension of the YLV graphical decomposition rules enables one to obtain efficient formulas for matrix elements of single generators and their products.

The graphical techniques unify several equivalent approaches to the quantum-mechanical many-body problem. The DRT treatment provides an optimal solution to the problem of representing the entire (or truncated) basis for each irrep. The YLV graphs enable one to express matrix elements in terms of quantities which possess group theoretical significance. In this respect this approach is more fundamental than the DRT method.

It is apparent that the use of graphical techniques as discussed herein may enable one to extend to $U(n)$ a variety of powerful techniques originally developed in the SU(2) regime. In this respect the utility of the unitary group approach as a single formalism which can treat arbitrary $U(n)$ problems is again emphasized. This latter point is of particular significance as the complexity of labeling increases.

ACKNOWLEDGMENTS

The support of the Natural Sciences and Engineering Research Council (NSERC) of Canada is gratefully acknowledged. One of us (M.S.) wishes to express his indebtedness to the late G. Racah.

[1]A. P. Yutsis, J. B. Levinson, and V. V. Vanagas, *Mathematical Apparatus of the Theory of Angular Momentum* (Israel Program for Scientific Translation, Jerusalem, 1962).

[2]D. M. Brink and G. R. Satchler, *Angular Momentum,* 2nd ed. (Clarendon, Oxford, 1968).

[3]I. M. Gel'fand and M. L. Zetlin, Dokl, Akad. Nauk SSSR **71**, 825, 1017 (1950).

[4]G. E. Baird and L. C. Biedenharn, J. Math. Phys. **4**, 1499 (1963); **5**, 1723 (1964); **5**, 1730 (1964); **6**, 1847 (1965).

[5]M. Moshinsky, *Group Theory and the Many-Body Problem* (Gordon and Breach, New York, 1968).

[6]L. C. Biedenharn, A. Giovannini, and J. D. Louck, J. Math. Phys. **8**, 691 (1967); L. C. Biedenharn and J. D. Louck, Commun. Math. Phys. **8**, 89 (1968); J. D. Louck and L. C. Biedenharn, J. Math. Phys. **11**, 2368 (1970).

[7]J. D. Louck, Am. J. Phys. **38**, 3 (1970).

[8]G. Racah, Phys. Rev. **62**, 438 (1942); **63**, 367 (1943); **76**, 1352 (1949).

[9]E. P. Wigner, in *Quantum Theory of Angular Momentum*, edited by L. C. Biedenharn and H. Van Dam (Academic, New York, 1965), pp. 87–133.

[10]L. C. Biedenharn and J. D. Louck, in *Angular Momentum in Quantum Physics: Theory and Application,* Vol. 8 in *Encyclopedia of Mathematics and Its Applications,* edited by G.-C. Rota (Addison-Wesley, Reading, MA, 1981).

[11]L. C. Biedenharn and J. D. Louck, in *The Racah-Wigner Algebra in Quantum Theory,* Vol. 9 in *Encyclopedia of Mathematics and Its Applications,* edited by G.-C. Rota (Addison-Wesley, Reading, MA, 1981).

[12]W. G. Harter, Phys. Rev. A **8**, 2819 (1973); W. G. Harter and C. W. Patterson, *A Unitary Calculus for Electronic Orbitals,* Vol. 49 of *Lecture Notes in Physics* (Springer-Verlag, Berlin, 1976).

[13]G. W. F. Drake and M. Schlesinger, Phys. Rev. A **15**, 1990 (1977).

[14]I. Shavitt, Int. J. Quantum Chem. **11S**, 131 (1977); **12S**, 5 (1978).

[15]J. Paldus, J. Chem. Phys. **61**, 5321 (1974). This work discusses the use of data compression techniques for expressing SU(2) Gel'fand tableaux in compact form using $L=2$ partitions of n, of particular relevance in quantum chemistry (see, for example, Ref. 5). Also, J. Paldus and M. J. Boyle, Phys. Scripta **21**, 295 (1980); M. J. Boyle and J. Paldus, Phys. Rev. A **22**, 2299 (1980); **22**, 2316 (1980).

[16]*The Unitary Group for the Evaluation of Electronic Energy Matrix elements,* Vol. 22 of *Lecture Notes in Chemistry,* edited by J. Hinze (Springer-Verlag, Berlin, 1981), Vol. 22.

[17]I. Shavitt, *Mathematical Frontiers in Computational Chemical Physics,* edited by D. G. Truhlar (Springer-Verlag, Berlin, 1988).

[18]R. D. Kent and M. Schlesinger, Int. J. Quantum Chem. **30**, 737 (1986); Comput. Phys. Commun. **43**, 413 (1987); J. Chem. Phys. **84**, 1583 (1986); Phys. Rev. A **36**, 4737 (1987). Also, see the article by S. Rettrup in Ref. 16.

[19]R. D. Kent, M. Schlesinger, and Pardu S. Ponnapalli, Phys. Rev. A **39**, 19 (1989); **39**, 3260 (1989).

[20]J. Q. Chen and M. J. Gao, J. Math. Phys. **23**, 928 (1982); J. Q. Chen and X. G. Chen, J. Phys. A **16**, 3435 (1983); J. Q. Chen, M. J. Gao, and X. G. Chen, J. Phys. A **17**, 481 (1984).

[21]J. Q. Chen, P. N. Wang, Z. M. Lu, and X. B. Wu, *Tables of the Clebsch-Gordan, Racah and Subduction Coefficients of SU(n) Groups* (World Scientific, Singapore, 1987). Also see H. A. Jahn, Phys. Rev. **96**, 989 (1954).

[22]C. R. Sarma and G. G. Sahasrabudhe, J. Math. Phys. **21**, 638 (1980).

[23]R. D. Kent and M. Schlesinger, Intern. J. Quantum Chem. **25**, 1111 (1984).

[24]R. D. Kent and M. Schlesinger, Phys. Rev. B **27**, 46 (1983); P. S. Ponnapalli, M. Schlesinger, and R. D. Kent *ibid.* **31**, 1258 (1985); R. D. Kent, M. Schlesinger, and P. S. Ponnapalli, *ibid.* **31**, 1264 (1985).

[25]R. D. Kent and M. Schlesinger, Phys. Rev. A **23**, 979 (1981).